Article (refereed) - postprint

Contact CEH NORA team at
noraceh@ceh.ac.uk

Relationship between critical load exceedances and empirical impact indicators at Integrated Monitoring sites across Europe

M. Holmberg[a], J. Vuorenmaa[a], M. Posch[b], M. Forsius[a], L. Lundin[c], S. Kleemola[a] , A. Augustaitis[d], B. Beudert[e], H.A. de Wit[f], T. Dirnböck[g], C.D. Evans[h], J. Frey[i], U. Grandin[c], I. Indriksone[j], P. Krám[k], E. Pompei[l], H. Schulte-Bisping[m], A. Srybny[n], M. Váňa[o]

[a]Finnish Environment Institute (SYKE), P.O. Box 140, FI-00251 Helsinki, Finland, Corresponding author: maria.holmberg@ymparisto.fi
[b]Coordination Centre for Effects (CCE), RIVM, P.O. Box 1, NL-3720 BA Bilthoven, The Netherlands
[c]Swedish University of Agricultural Sciences, P.O. Box 7050, SE-75007 Uppsala, Sweden
[d]Forest Monitoring Laboratory, Aleksandras Stulginskis University, Studentu 13, Kaunas distr. LT-53362, Lithuania
[e]Bavarian Forest National Park, Freyunger Str. 2, D-94481 Grafenau, Germany
[f]Norwegian Institute for Water Research (NIVA), Gaustadalléen 21, NO-0349 Oslo, Norway
[g]Environment Agency Austria, Spittelauer Lände 5, A-1090 Vienna, Austria
[h]Centre for Ecology and Hydrology (CEH), Environment Centre Wales, Deiniol Road, Bangor, LL61 6HJ, U.K.
[i]Tartu University, Institute of Ecology and Earth Sciences, Vanemuise St. 46, EE-51014 Tartu, Estonia
[j]State Ltd Latvian Environment, Geology and Meteorology Centre, 165 Maskavas Str., LV-1019 Riga, Latvia
[k]Czech Geological Survey, Department of Geochemistry, Klarov 3, CZ-118 21 Prague 1, Czech Republic
[l]National Forest Service (Div. VI), CONECOFOR, Via Carducci 5, I-00187 Rome, Italy
[m]University of Göttingen, Inst Soil Science & Forest Nutrition, D-37077 Göttingen, Germany
[n]Berezinsky Biosphere Reserve, P.O Domzheritzy, Lepel District, Vitebskaya oblast, 211188, Belarus
[o]Czech Hydrometeorological Institute, Observatory Košetice, CZ-394 22 Košetice, Czech Republic

Abstract

Critical loads for acidification and eutrophication and their exceedances were determined for a selection of ecosystem effects monitoring sites in the Integrated Monitoring programme (UNECE ICP IM). The level of protection of these sites with respect to acidifying and eutrophying deposition was estimated for 2000 and 2020. In 2020 more sites were protected from acidification (67 %) than in 2000 (61%). However, due to the sensitivity of the sites, even the maximum technically feasible emission reductions scenario would not protect all sites from acidification. In 2000, around 20% of the IM sites were protected from eutrophication. In 2020, under reductions in accordance with current legislation, about one third of the sites would be protected, and at best, with the maximum technically feasible reductions, half of the sites would be protected from eutrophication. Data from intensively monitored sites, such as those in ICP IM, provide a connection between modelled critical thresholds and empirical observations, and thus an indication of the applicability of critical load estimates for natural ecosystems. Across the sites, there was good correlation between the exceedance of critical loads for acidification and key acidification parameters in runoff water, both with annual mean fluxes and concentrations. There was also evidence of a link between exceedances of critical loads of nutrient nitrogen and nitrogen leaching. The collected empirical data of the ICP IM thus allow testing and validation of key concepts used in the critical load calculations. This increases confidence in the European-scale critical loads mapping used in integrated assessment modelling to support emission reduction agreements.

1. Introduction

Critical loads are deposition thresholds used to describe the sensitivity of ecosystems to air-borne pollution. A critical load is defined as "a quantitative estimate of an exposure to one or more pollutants below which significant harmful effects on specified sensitive elements of the environment do not occur according to present knowledge" (Nilsson and Grennfelt, 1988). The

lower the critical load, the more sensitive the ecosystem is considered to be. The critical loads and levels approach for pollution control has gathered momentum over the past two decades, and has been successfully used in strategies for emission reductions under the United Nations Economic Commission for Europe (UNECE) Convention on Long-range Transboundary Air Pollution (LRTAP) and the EU National Emission Ceilings Directive (Hettelingh et al., 2007; Amann et al., 2011).

The integrated assessment of emissions and effects of air pollutants relies on critical loads for acidification and eutrophication to quantify risks of ecosystem damage. In 2000, 12% of the ecosystem area in Europe was at risk of acidification and 54% at risk of eutrophication, according to an analysis based on critical loads (Hettelingh et al., 2011). Critical loads have also been used to assess impacts of air pollutants in North America (Ouimet et al., 2006; Pardo et al., 2011) and in the Arctic and Sub-Arctic (Forsius et al., 2010).

Empirical scientific evidence based on environmental monitoring programmes is essential for documenting the ecosystem benefits of costly emission reduction policies. The multidisciplinary International Cooperative Programme of Integrated Monitoring (UNECE ICP IM) under the LRTAP Convention quantifies pollutant effects on the environment through monitoring, modelling and scientific review, using data from catchments/plots located in predominantly forested natural or semi-natural areas (ICP IM Manual, 1998; Forsius et al., 2001; Forsius et al., 2005). Results of ICP IM provide a valuable means to study the link between critical thresholds of acidification and eutrophication of ecosystems and empirical impact indicators.

This paper has two aims: i) to calculate site-specific critical loads and their exceedances for acidification and eutrophication for terrestrial and aquatic ecosystems at selected European ICP IM sites using mass balance methods and empirical values of critical loads of nutrient nitrogen, and modelled historical and future sulphur (S) and nitrogen (N) depositions; and ii) to present relationships between the exceedances of critical loads and empirical impact indicators evaluated on the basis of surface water chemistry measurements at IM sites.

2. Materials and methods

2.1 Critical loads for acidification

In this study, the Steady-State Water Chemistry (SSWC) model embedded into the First-order Acidity Balance (FAB) model (Henriksen and Posch, 2001; UBA, 2004) was used to calculate critical loads for 18 ICP IM catchments for which observations of runoff volume and water chemistry were available for the years evaluated (Fig. 1, Table 1). This is an extension of previous work, which calculated critical loads of acidification for 16 ICP IM catchments using the SSWC model only (Holmberg et al. 2010). Mean values of observed concentrations (sulphate, nitrate, calcium, magnesium, potassium, sodium, chloride) for the period 2000-2002 were used in the calculations.

In the FAB model, critical loads of N and S acidity are derived in the same way as in the Simple Mass Balance model, widely used for computing soil critical loads (Sverdrup and De Vries, 1994; UBA, 2004). Starting from the charge balance in the lake or stream water and using steady-state mass balances of N, S and base cations, one arrives at the following equation (Henriksen and Posch, 2001):

(1) $\qquad (1-\rho_S) \cdot S_{dep} + (1-\rho_N) \cdot b_N \cdot N_{dep} = (1-\rho_N) \cdot M_N + L_{crit}$,

where ρ_S and ρ_N represent in-lake retention of S and N, and L_{crit} is the difference between the net base cation leaching and the critical ANC leaching.

Every pair (N_{dep}, S_{dep}) of N and S deposition fulfilling this equation is called a critical load of acidity of that catchment. The dimensionless coefficient b_N and the flux M_N depend on N_{dep}: If $N_{dep} \leq N_u+N_i$, i.e. the N deposition is smaller than the sum of net uptake N_u and net immobilization N_i of N in the terrestrial catchment, then $M_N = 0$ and $b_N = r$, where r is the lake-to-catchment area ratio, reflecting the fact that only the N deposited directly onto the lake contributes to leaching. If, however, $N_{dep} > N_u+N_i$, then $M_N = (1–f_{de}) \cdot (1–r) \cdot (N_u+N_i)$ and $b_N = 1–(1–r) \cdot f_{de}$, where f_{de} is the fraction of N input denitrified. The critical loads of acidity define a trapezoidally-shaped function in the (N_{dep}, S_{dep})-plane, called the critical load function (see Figure 2), defined by the maximum critical load of S, $CL_{max}S$ (if $N_{dep} = 0$) and the maximum critical load of N, $CL_{max}N$ (for $S_{dep} = 0$).

It was assumed that there is no permanent removal of biomass from the integrated monitoring sites as they are located in protected areas with no significant management. Therefore the rate of net nitrogen uptake N_u from the soil was set to zero at all sites, since nitrogen incorporated into growing vegetation was considered to be balanced, in the long term, by nitrogen released from decaying litter. A constant N immobilization in the catchment soils of $N_i = 0.5$ kg N ha^{-1}a^{-1} was used (UBA, 2004). The denitrification fraction in the catchment soils was estimated as $f_{de} = 0.1+0.7 \cdot f_{peat}$, where f_{peat} is the fraction of peatlands in the terrestrial catchment (after Posch et al., 1997). The values of f_{peat} are given in Table A1 of the Supplementary material. The dimensionless quantities ρ_N and ρ_S account for the in-lake retention of N and S respectively. The retention factor for N is modelled following Kelly et al. (1987): $\rho_N = s_N/(s_N+Q/r)$, where s_N is the net mass transfer coefficient. A value of $s_N = 6.5$ m yr^{-1} was chosen for all lakes using data from Kaste and Dillon (2003). An analogous equation describes ρ_S, and $s_S = 0.5$ m yr^{-1} was used for all lakes (after Baker and Brezonik, 1988).

The term L_{crit} in the critical load equation denotes the difference between the net base cation leaching and the critical ANC leaching. Since the base cation fluxes, especially those due to weathering in the catchment soils, are poorly known, this term is modelled by the SSWC model (Henriksen and Posch, 2001), i.e.:

(2) $\qquad L_{crit} = Q \cdot ([BC^*]_0 - [ANC]_{limit})$,

from catchment runoff Q (m yr^{-1}), pre-acidification non-marine concentration of base cations $[BC^*]_0$ (µeq L^{-1}) (BC=Ca+Mg+K+Na) and a critical acid neutralizing capacity $[ANC]_{limit}$ (µeq L^{-1}). The criterion is the lowest acid neutralizing capacity that does not damage target biota (fish). The value $[ANC]_{limit} = 20$ µeq L^{-1} was used in this study (Lien et al., 1996). The pre-acidification base cation concentration is calculated as (Henriksen and Posch, 2001):

(3) $\qquad [BC^*]_0 = [BC^*] - F ([SO_4^*] - [SO_4^*]_0 + [NO_3])$,

where the pre-acidification concentration of sulphate is estimated as $[SO_4^*]_0 = a + b \cdot [BC^*]$, with $a = 8$ µeq L^{-1}, $b = 0.17$, and the so-called F-factor is computed as (Brakke et al., 1990):

(4) $\qquad F= \sin(\pi/2[BC^*]/[S])$,

with $[S] = 400$ µeq L^{-1}.

2.2 Critical loads for eutrophication

Deposition of nitrogen may have an impact on sensitive ecosystems through multiple pathways, including accumulation of N compounds, resulting in changes of species composition and reduction in plant diversity as well as increased susceptibility to secondary stress and disturbance factors such as drought, frost, pathogens or herbivores (Achermann and Bobbink, 2003; Phoenix et al., 2006; Nordin et al., 2006; Salemaa et al., 2008; Bobbink and Hettelingh, 2011; Pardo et al., 2011).

Mass balance critical loads of nutrient nitrogen $CL_{nut}N$ (eq ha^{-1}yr^{-1}) were calculated for the same 18 catchments for which observations of runoff volume and water chemistry were available for the evaluated years (Fig. 1). Critical loads of nutrient nitrogen were calculated with an N budget equation that describes the amount of N deposition the terrestrial ecosystem may receive without increasing the soil solution N concentration above a specified limit $[N]_{acc}$

(5) $CL_{nut}N = N_i + N_u + Q\,[N]_{acc}\,/\,(1–f_{de}),$

where N_i is the long-term net immobilisation of N in the soil, N_u is the net removal of N in harvested vegetation, f_{de} is the fraction of N input denitrified and Q the annual runoff (see above). The acceptable N concentration $[N]_{acc}$ in soil leachate is set to avoid nutrient imbalances or vegetation changes, (UBA 2004, De Vries et al. 2007). In this study, site-specific values for $[N]_{acc}$ (0.3 to 5.2 mgN L^{-1}) were chosen to reflect the sensitivity of part of the vegetation of the site (Table A1, supplementary material).

In addition to the above mass balance critical loads of nutrient N, empirical critical loads of nutrient N, $CL_{emp}N$, were also assigned to a total of 83 vegetation plots at 37 IM sites (Fig. 1). This was based on the work by Bobbink and Hettelingh (2011), who reported critical loads of nutrient N from extensive empirical studies on the response of natural and semi-natural ecosystems to N deposition. The empirical critical loads of N are given for the groups of natural and semi-natural ecosystems, which have been classified according to the EUNIS (European Nature Information System) habitat classification for Europe (Davies et al., 2004). On the basis of information on the vegetation reported for the plots of the Integrated Monitoring sites, the individual plots were classified into EUNIS classes. For each EUNIS class the empirical critical load was set to the minimum of the range proposed by Bobbink and Hettelingh (2011). In this analysis, site-specific factors that modify the empirical values were not considered, in contrast to the practice of some of the individual countries in their reporting to the CCE; e.g. in the UK, the reported empirical critical loads vary with the amount of rainfall (Hall et al., 2011). The values of the $CL_{emp}N$ range from 5 to 15 kg N ha^{-1}yr^{-1} (360 to 1070 eq ha^{-1}yr^{-1}) (Table A1, Supplementary material).

2.3 Deposition estimates and critical load exceedances

The deposition estimates were generated with the source-receptor matrices – derived from the EMEP/MSC-W unified atmospheric dispersion model (EMEP 2010) – used in integrated assessment under the LRTAP Convention (Amann et al. 2010) using the NAT2000, COB2020, Low*2020, MID2020, High*2020 and MFR2020 emission scenarios. The NAT2000 scenario represents historic emissions for the year 2000 and the COB2020 scenario national economic projections for 2020 as reported by the countries under the LRTAP Convention. The Low*2020 and High*2020 scenarios refer to the ambition level of the reductions, so that with lower reductions the scenario Low*2020 leads to more deposition than High*2020. The Low*2020, MID2020 and High*2020 scenarios are based on economic projections by the PRIMES model for the year 2020,

and MFR2020 assumes all available abatement technologies being implemented by 2020. The depositions were available for $50 \times 50 \text{km}^2$ grid cells covering Europe.

The increased risk for harmful effects is quantified by the exceedance of a critical load. For nutrient N critical loads, the exceedance is defined as the difference between the N deposition and the critical load value. Negative exceedance values (for sites where the critical loads are not exceeded) are included in graphs in order to show the difference between deposition and critical load value for all cases.

In the case of acidification, both N and S contribute to the exceedance, and there are, in general, infinitely many ways of reducing deposition so that the critical loads are no longer exceeded. It has become customary to define the exceedance as the sum of the N and S deposition reduction required to reach the critical load function on the shortest path (Posch et al., 2001; UBA, 2004): $Ex(N_{dep}, S_{dep}) = \Delta N + \Delta S$ (see Figure 2). If (N_{dep}, S_{dep}) lies below the critical load function, the critical loads are not exceeded.

For empirical critical loads of nutrient N, a site was considered protected from eutrophication if all the vegetation habitats within the site were protected (N_{dep} lower than $CL_{emp}N$). For each site, the exceedance of $CL_{emp}N$ was calculated as a habitat-specific area-weighted average value. Exceedance averages were calculated as arithmetic means of the positive exceedance values over the number of sites at which the critical loads were exceeded ($AExCL_A$, $AExCL_{nut}N$, $AExCL_{emp}N$, all in eq ha^{-1} yr^{-1}).

2.4 Empirical impact indicators

For the study of chemical empirical impact indicators in relation to exceedance of critical loads of acidification ($ExCL_A$), 17 catchments were selected (Table 1). The selection of catchments was guided by the availability of surface water chemistry and runoff data in the ICP IM database. At these same catchments, the mass balance critical loads of nutrient N ($ExCL_{nut}N$) were compared with fluxes of total inorganic nitrogen (TIN = $NO_3^- + NH_4^+$) (Table 2). In addition, the empirical critical loads of nutrient N ($ExCL_{emp}N$) were investigated in relation to observed monitoring results (empirical impact indicators) at a total of 24 sites, in which surface water concentration data of TIN were available (Table 2). A list of the National Focal Points contributing runoff chemistry data is available at the web site of the ICP IM (ICP IM network, 2011).

The exceedances of critical loads were computed with the historical deposition estimates NAT2000. To compare catchment responses with exceedances of critical loads at the IM catchments, the annual average (2000 – 2002) runoff water fluxes and concentrations of the key acidification parameters acid neutralising capacity ANC, hydrogen-ion (H$^+$) and non-marine sulphate (xSO$_4$), and eutrophication parameter TIN were used as empirical impact indicators. Acid neutralising capacity ANC was calculated as $(Ca^{2+} + Mg^{2+} + Na^+ + K^+) - (SO_4^{2-} + Cl^- + NO_3^-)$. The period 2000-2002 was used to be consistent with the deposition estimates (NAT2000). Annual runoff water element fluxes were calculated by summing mean monthly fluxes, obtained from monthly mean water flux and monthly mean solute concentration. Methods for collection, storage and analysis are described in the ICP IM Manual (1998).

The empirical impact indicators were compared with critical load exceedances by correlation analysis. The correlation of runoff water concentrations and fluxes on the exceedances of critical loads was examined using non-parametric Kendall-tau correlation analysis (Conover, 1980). The

sites BY02, DE01 and EE02 were excluded from the comparison between exceedance of critical load of N and TIN runoff water chemistry. High concentrations and fluxes of TIN at sites BY02 and EE02 are due to inputs of N from agriculture, and for site DE01 due to excess mineralization after Norway spruce (*Picea abies*) dieback due to a bark beetle attack in 1996-1997, and are therefore not considered representative of the effect of N deposition.

3. Results and discussion

3.1 Acidification

The ICP IM catchments vary in their sensitivity to acidification. Based on the surface water chemistry, 4 out of 18 sites can be characterized as acid-sensitive (ANC ≤ 20 µeq L^{-1}), and for these sites the critical load of acidity was exceeded in 2000. The acid-sensitive sites are also characterized by high acidity (pH < 5) of the surface water. Surface waters with an ANC over 200 µeq L^{-1}, on the other hand, are considered to be insensitive to acidification, and this is the case for about 40% of the sites (Table 1).

More than half of the sites were protected from surface water acidification in 2000; 11 sites out of 18, or 61% (Tables 1, 3). For all deposition scenarios in 2020, 12 sites (67%) were protected from acidification. Even the high ambition High*2020 or MFR2020 scenarios would not protect the remaining 6 sites: CZ01, CZ02, NO01, SE04, SE14, SE15. Arithmetic averages were calculated for the exceedance of critical loads of acidity for the sites that were not protected from acidification (7 in 2000; 6 in 2020). The average exceedance (for the exceeded sites only) decreased from 987 eq ha^{-1} yr^{-1} in 2000 to 310 eq ha^{-1} yr^{-1} in 2020, for the maximum feasible reductions MFR2020 scenario (Table 3).

There was good correlation between the exceedances of acidity critical loads ($ExCL_A$) and key acidification parameters in runoff water, both in annual mean fluxes and concentrations (Fig. 3, Table 4). At the most acidified or acid-sensitive sites (in terms of low ANC and high H$^+$ concentrations and fluxes), the sulphur deposition exceeded critical loads for acidification to a higher degree than at other, less sensitive sites. At lower deposition levels, these sites were closer to the exceedance threshold than the sensitive sites. The correlation between sulphate and $ExCL_A$ among the IM sites was poorer, due to differences in soil susceptibility to acidification. Some sites (EE02, LT01, LT03, LV01, LV02) are located in deep calcareous soils with high initial concentrations of sulphate, calcium and magnesium, and high concentrations of ANC (> 1000 µeq L^{-1}, n=9), and are therefore well protected against acidification (Table 1). Among the acid-sensitive sites (ANC < 100 µeq L^{-1}) $ExCL_A$ increases with increasing sulphate flux (Kendall τ b correlation coefficient 0.67, p < 0.05) (Fig. 4).

Much has been achieved in reducing European emissions of S (and to a lesser extent N) during the last decades. Between 1990 and 2009, European emissions of SO$_x$, NO$_x$ and NH$_3$ have been reduced by 73 %, 36 % and 31 %, respectively (Fagerli et al., 2011). The resulting decreases in acidifying deposition, and consequently reduced CL exceedances, have led to well-documented recovery in ecosystems, regarding both chemical (e.g. Stoddard et al., 1999; Evans et al., 2001; Wright et al., 2005) and to a lesser extent biological indicators (e.g. Snucins et al., 2001; Skjelkvåle and de Wit, 2011). Dynamic model calculations show that further improvements are likely to occur if the planned reductions are implemented (Aherne et al., 2008; Larssen et al., 2010, Oulehle et al., 2012).

3.2 Eutrophication

At 14 IM sites of 18 examined in this study, the mass balance critical load of nutrient nitrogen ($CL_{nut}N$) was exceeded in 2000 (NAT2000) (Tables 2, 3), i.e. only 4 sites (22%) were protected from eutrophication in 2000. In 2020 the current reduction plans COB2020 and the low ambition Low*2020 scenarios would protect 5 sites, while the high ambition High*2020 and the MFR scenario would protect 7 sites from eutrophication. The average exceedance of the mass balance critical load of nutrient nitrogen was 625 eq ha^{-1} yr^{-1} or 8.8 kg N ha^{-1} yr^{-1} in 2000 and 230 eq ha^{-1} yr^{-1} or 3.2 kg N ha^{-1} yr^{-1} in 2020 under the MFR scenario N deposition (Table 2).

From the perspective of using the empirical critical loads of nitrogen ($CL_{emp}N$) as an indicator of nitrogen tolerance, 7 sites of 37 (19%) were protected from eutrophication in 2000 (Tables 2, 3). In 2020, the mid and high ambition scenarios protected 15 sites, whereas 20 sites would be protected if all available abatement technologies were implemented (MFR). The average exceedance of the empirical critical load of nitrogen was 578 eq ha^{-1} yr^{-1} or 8.1 kg N ha^{-1} yr^{-1} in 2000 and 154 eq ha^{-1} yr^{-1} or 2.2 kg N ha^{-1} yr^{-1} in 2020 under the MFR scenario N deposition (Table 3).

There was good agreement between exceedances of critical loads of nitrogen and observed N leaching (Table 4, Fig. 5). The ICP IM sites where the empirical critical load of nutrient nitrogen ($CL_{emp}N$) was exceeded showed higher TIN concentrations and fluxes in runoff. With the NAT2000 deposition scenario, the empirical critical load of nutrient nitrogen ($CL_{emp}N$) was exceeded at 18 (75%) sites of those for which TIN concentrations were available (24 sites). For those 17 sites where TIN fluxes were available, $CL_{emp}N$ was exceeded at 14 sites (82 %) (Fig. 5). The concentrations and fluxes of TIN increased with increasing critical load exceedance also regarding mass balance nutrient N critical loads ($CL_{nut}N$).

Empirical data from forested ecosystems in Europe show a clear relationship between N deposition and N leaching (Dise and Wright, 1995, Wright et al., 2001, MacDonald et al., 2002, Kaste et al., 2007). Dise and Wright (1995) and Wright et al. (2001) observed low concentrations of nitrate in stream water at sites with less than 10 kg N ha^{-1} yr^{-1} deposition, elevated concentrations at sites receiving more than 25 kg N ha^{-1} yr^{-1} and variable responses in the mid-range. In our study, N deposition was less than 25 N ha^{-1} yr^{-1} at all catchments and NO$_3$-N constituted on average 79% of the TIN in stream water 2000-2002. The highest TIN fluxes were observed at catchments receiving more than 7 kg N ha^{-1} yr^{-1} in deposition (Fig. 6).

In contrast to sulphur, nitrogen is much more influenced by biological processes within ecosystems, and most of the N deposition is usually retained in forest ecosystems; typically < 10% is leached in runoff of boreal forest ecosystems, mostly as NO$_3$ (e.g. Wright et al., 2005). Furthermore, increasing temperature and availability of both CO$_2$ and N have stimulated forest growth (Spiecker et al., 1996) and N uptake from the soils (Johnson, 2006). Hence changes in N deposition may not always directly correlate with changes in inorganic N leaching. The variation in the relationship between N concentrations and fluxes and exceedances of critical loads may be expected, since N leaching depends on landscape characteristics, site history, soil fertility and organic matter pool, vegetation type and hydrological processes (Helliwell et al., 2007; Rothwell et al., 2008). However, continued high N deposition may result in N saturation of terrestrial ecosystems in the long run and excess NO$_3$ leaching to surface waters (e.g. Aber et al., 1989, Dise and Wright, 1995, MacDonald et al., 2002). There are still large uncertainties regarding the processes controlling N retention in ecosystems, and further research is required to narrow them down.

As time is not a variable in critical load calculations, critical loads represent the threshold beyond which effects on the ecosystems might occur, without regard to the time frame in which the effects might appear. Critical loads represent a static view of ecosystems, while in reality changing climate,

growing vegetation, and accumulation and release of elements into soil and organic matter, lead to dynamic responses of the ecosystems to changing deposition levels. A site could be exceeded but not yet damaged, or no longer exceeded but not yet recovered. Dynamic models are used to study these and other aspects (e.g. Jenkins et al., 2003, Hettelingh et al., 2007). In this paper we have compared exceedances of steady-state critical loads with empirical impact indicator observations as a snapshot of dynamically changing ecosystems. The comparison is relevant and our results provide evidence on the link between critical loads and empirical impacts. The coincidence of exceedance with effects is, however, neither a sufficient nor necessary condition for the validation of critical loads.

4. Conclusions

Although much has been achieved with regard to the reduction of acidifying deposition, only 61% of the ICP IM catchments studied here were protected from acidification in 2000 and emission reductions envisaged for 2020 would increase the level of protection to only 67 %. For eutrophication, the situation is more severe, only about 20% of the catchments were protected in 2000 and 39 % or 54 % would be protected in 2020, depending on whether mass balance or empirical critical loads of N are considered.

Empirical impact indicators as derived from observations at ICP IM catchments were in good agreement with exceedances of critical loads of acidification and eutrophication. Data from the ICP IM thus provide evidence of a connection between modelled critical loads and empirical monitoring results for acidification parameters and nutrient nitrogen. This increases the confidence in the European-scale critical loads mapping used in integrated assessment modelling.

References
Aber, J.D., Nadelhoffer, K.J., Steudler, P., Melillo, J.M., 1989. Nitrogen saturation in northern forest ecosystems. Biosci. 39, 378-386.

Achermann, B., Bobbink, R., 2003. Empirical critical loads for nitrogen. Proceedings from the expert workshop in Bern, Switzerland, Nov 11-13 2002. Environmental Documentation no 164 air. Swiss Agency for the Environment, Forest and Landscape.

Aherne, J., Posch, M., Forsius, M., Vuorenmaa, J., Tamminen, P., Holmberg, M., Johansson, M., 2008. Modelling the hydrogeochemistry of acid-sensitive catchments in Finland under atmospheric deposition and biomass harvesting scenarios. Biogeochem. 88, 233-256.

Amann, M., Bertok, I., Cofala, J., Heyes, C., Klimont, Z., Rafaj, P., Schöpp, W., Wagner, F., 2010. Scope for further environmental improvements in 2020 beyond the baseline projections. Background paper for the 47th Session of the Working Group on Strategies and Review of the Convention on Long-range Transboundary Air Pollution. Geneva 30.8.-3.9.2010. CIAM Report 1/2010, International Institute for Applied Systems Analysis, Laxenburg, Austria.

Amann, M., Bertok, I., Borken-Kleefeld, J., Cofala, J., Heyes, C., Höglund-Isaksson, L., Klimont, Z., Nguyen, B., Posch, M., Rafaj, P., Sandler, R., Schöpp, W., Wagner, F., Winiwarter, W., 2011. Cost-effective control of air quality and greenhouse gases in Europe: Modeling and policy applications. Env. Model. Softw. 26, 1489-1501.

Baker, L.A., Brezonik, P.L., 1988. Dynamic model of in-lake alkalinity generation. Water Resour. Res. 24(1), 65-74.

Bobbink, R., Hettelingh, J.P., 2011. Review and revision of empirical critical loads and dose-response relationships. Proceedings of an expert workshop, Noordwijkerhout 23-24 June 2010. Report 680359002, RIVM, Bilthoven, The Netherlands.

Brakke, D.F., Henriksen, A., Norton, S.A., 1990. A variable F-factor to explain changes in base cation concentrations as a function of strong acid deposition. Verh. Internat. Verein Limnol. 24, 146-149.

Conover, W.J., 1980. Practical Non-Parametric Statistics, second ed. John Wiley and Sons, New York.

Davies, C.E., Moss, D., Hill, M.O., 2004. EUNIS habitat classification revised 2004, European Topic Centre on Nature Protection and Biodiversity. http://eunis.eea.europa.eu/references/1473 http://eunis.eea.europa.eu/upload/EUNIS_2004_report.pdf (accessed 7.6.2012).

De Vries, W., Kros, H., Reinds, G.J., Wamelink, W., Mol, J., Van Dobben, H., Bobbink, R., Emmett, B., Smart, S., Evans, C., Schlutow, A., Kraft, P., Belyazid, S., Sverdrup, H., Van Hinsberg, A., Posch, M., Hettelingh, J.-P., 2007. Developments in deriving critical limits and modelling critical loads of nitrogen for terrestrial ecosystems in Europe. Alterra-report 1382. Alterra, Wageningen and CCE, Bilthoven, The Netherlands.

Dise, N.B., Wright, R.F., 1995. Nitrogen leaching from European forests in relation to nitrogen deposition. Forest Ecology Management 71, 153-161.

EMEP, 2010. www.emep.int/mscw/index_mscw.html. (accessed 7.6.2012)

Evans, C.D., Cullen, J.M., Alewell, C., Kopácek, J., Marchetto, A., Moldan, F., Prechtel, A., Rogora, M., Veselý, J., Wright, R., 2001. Recovery from acidification in European surface waters. Hydrol. Earth Syst. Sci. 5(3), 283-297.

Fagerli, H., Gauss, M., Benedictow, A., Griesfeller, J., Jonson, J.E., Nyíri, Á. et al., 2011. Transboundary Acidification, Eutrophication and Ground Level Ozone in Europe in 2009. EMEP Status Report 2011. Norwegian Meteorological Institute. Oslo.

Forsius, M., Kleemola, S., Vuorenmaa, J., Syri, S., 2001. Fluxes and trends of nitrogen and sulphur compounds at Integrated Monitoring Sites in Europe. Water, Air, Soil Poll. 130, 1641-1648.

Forsius, M., Kleemola, S., Starr, M., 2005. Proton budgets for a monitoring network of European forested catchments: impacts of nitrogen and sulphur deposition. Ecol. Indicators 5, 73-83.

Forsius, M., Posch, M., Aherne, J., Reinds, G.J., Christensen, J., Hole, L., 2010. Assessing the impacts of long-range sulfur and nitrogen deposition on arctic and sub-arctic ecosystems. Ambio 39, 136-147.

Hall, J., Emmett, B., Garbutt, A., Jones, L., Rowe, E., Sheppard, L., Vanguelova, E., Pitman, R., Britton, A., Hester, A., Ashmore, M., Power, S., Caporn, S., 2011. UK Status Report July 2011: Update to empirical critical loads of nitrogen. http://cldm.defra.gov.uk/PDFs/UK_status_report_2011_finalversion_July2011_v2.pdf. (accessed 7.6.2012)

Henriksen, A., Posch, M., 2001. Steady-state models for calculating critical loads of acidity for surface waters. Water, Air, Soil Poll. Focus 1, 375-398.

Helliwell, R.C., Coull, M.C., Davies, J.J.L., Evans, C.D., Norris, D., Ferrier, R.C., Jenkins, A., Reynolds, B., 2007. The role of catchment characteristics in determining surface water nitrogen in four upland regions in the UK. Hydrol. Earth Syst. Sci. 11(1), 256-271.

Hettelingh, J.-P., Posch, M., Slootweg, J., Reinds, G.J., Spranger, T., Tarrason, L., 2007. Critical loads and dynamic modelling to assess European areas at risk of acidification and eutrophication. Water, Air, Soil Poll. Focus 7, 379-384.

Hettelingh, J.-P., Posch, M., Slootweg, J., Le Gall, A.-C., 2011. Revision of the Gothenburg Protocol: Environmental Effects of GAINS Scenarios Developed during Summer 2011. In: Posch, M., Slootweg, J., Hettelingh, J.-P. (Eds.) Modelling Critical Thresholds and Temporal Changes of Geochemistry and Vegetation Diversity. CCE Status Report 2011. Coordination Centre for Effects, Bilthoven, The Netherlands, pp 13-27.

Holmberg, M., Posch, M., Kleemola, S., Vuorenmaa, J., Forsius, M., 2010. Calculation of site-specific critical loads for acidification and eutrophication for terrestrial and aquatic ecosystems. In: Kleemola, S. and Forsius, M. (Eds.) Convention on Long-range Transboundary Air Pollution International Cooperative Programme on Integrated Monitoring of Air Pollution Effects on Ecosystems. 19th Annual Report 2010. Working Group on Effects of the CLTRAP. Finnish Environment Institute, Helsinki, pp. 27-36.

ICP IM Manual, 1998. Finnish Environment Institute, Helsinki. http://www.environment.fi/default.asp?node=6329&lan=en. (accessed 7.6.2012)

ICP IM network, 2011. www.environment.fi/default.asp?node=6328&lan=en. (accessed 7.6.2012)

Jenkins, A., Cosby, B.J., Ferrier, R.C., Larssen, T., Posch, M., 2003. Assessing emission reduction targets with dynamic models: deriving target load functions for use in integrated assessment. Hydrol. Earth Syst. Sci. 7(4), 609-617.

Johnson, D.W., 2006. Progressive N limitation in forests: Review and implications for long-term responses to elevated CO_2. Ecology, 87(1), 64-75.

Kaste, Ø., Dillon, P.J., 2003. Inorganic nitrogen retention in acid-sensitive lakes in southern Norway and southern Ontario, Canada - a comparison of mass balance data with an empirical N retention model. Hydrol Proc. 17, 2393-2407.

Kaste, Ø., De Wit, H., Skjelkvåle, B.L., Høgåsen, T., 2007. Nitrogen runoff at ICP Waters sites 1990-2005: Increasing importance of confounding factors? In: De Wit, H., Skjelkvåle, B.L. (Eds.), Trends in surface water chemistry and biota; the importance of confounding factors. ICP Waters Report 87/2007, Norwegian Institute for Water Research, Oslo; 2007. pp. 29-38.

Kelly, C.A., Rudd, J.W.M., Hesslein, R.H., Schindler, D.W., Dillon, P.J., Driscoll, C.T., Gherini, S.A., Hecky, R.E., 1987. Prediction of biological acid neutralization in acid-sensitive lakes. Biogeochem. 3, 129-140.

Larssen, T., Cosby, B.J., Lund, E., Wright, R.F., 2010. Modeling future acidification and fish populations in Norwegian surface waters. Environ. Sci. Technol. 44, 5345–5351

Lien, L., Raddum, G.G., Fjellheim, A., Henriksen, A., 1996. A critical limit for acid neutralizing capacity in Norwegian surface waters, based on new analyses of fish and invertebrate responses. Sci. Total Environ. 177, 173-193

MacDonald, J.A., Dise, N.B., Matzner, E., Armbruster, M., Gundersen, P., Forsius, M., 2002. Nitrogen input together with ecosystem nitrogen enrichment predict nitrate leaching from European forests. Global Change Biology. 8, 1028-1033.

Nilsson, J., Grennfelt, P., 1988. Critical loads for sulphur and nitrogen. Miljørapport 1988:15. Nordic Council of Ministers, Copenhagen.

Nordin, A., Strengbom, J., Ericson, L., 2006. Responses to ammonium and nitrate additions by boreal plants and their natural enemies. Environ. Poll. 141,167-174.

Oulehle, F., Cosby, B.J., Wright, R.F., Hruška, J., Kopáček, J., Krám, P., Evans, C.D., Moldan, F., 2012. Modelling soil nitrogen: The MAGIC model with nitrogen retention linked to carbon turnover using decomposer dynamics. Environ. Poll. 165, 158-166.

Ouimet, R., Arp, P.A., Watmough, S.A., Aherne, J., Demerchant I., 2006. Determination and mapping critical loads of acidity and exceedances for upland forest soils in Eastern Canada. Water, Air, Soil Poll. 172, 57-66.

Pardo, L.H., Fenn, M.E., Goodale, C.L., Geiser, L.H., Driscoll, C.T., Allen, E.B., Baron, J.S., Bobbink, R., Bowman, W.D., Clark, C.M., Emmett, B., Gilliam, F.S., Greaver, T.L., Hall, S.J.,

Lilleskov, E.A., Liu, L., Lynch, J.A., Nadelhoffer, K.J., Perakis, S.S., Robin-Abbott, M.J., Stoddard, J.L., Weathers, K.C., Dennis, R.L., 2011. Effects of nitrogen deposition and empirical nitrogen critical loads for ecoregions of the United States. Ecological Applications 21(8), 3049-3082.

Phoenix, G.K., Hicks, W.K., Cinderby, S., Kuylenstierna, J.C.I., Stock, W.D., Dentener, F.J., Giller, K.E., Austin, A.T., Lefroy, R.D.B., Gimeno, B.S., Ashmore, M.R., Ineson, P., 2006. Atmospheric nitrogen deposition in world biodiversity hotspots: the need for a greater global perspective in assessing N deposition impacts. Global Change Biology 12(3), 470-476.

Posch, M., Kämäri, J., Forsius, M., Henriksen, A., Wilander, A., 1997. Exceedance of critical loads for lakes in Finland, Norway and Sweden: Reduction requirements for acidifying nitrogen and sulfur deposition. Environ. Management. 21(2), 291-304

Posch, M., Hettelingh, J.-P., De Smet, P.A.M., 2001. Characterization of critical load exceedances in Europe. Water, Air, Soil Poll. 130, 1139-1144.

Rothwell, J.J., Futter, M.N., Dise, N.B., 2008. A classification and regression tree model of contols on dissolved inorganic nitrogen leaching from European forests. Environ Poll. 156, 544-552.

Salemaa, M., Mäkipää, R., Oksanen, J., 2008. Differences in the growth response of three bryophyte species to nitrogen. Environ Poll. 152, 82-91.

Skjelkvåle, B.L., De Wit, H., 2011. Trends in precipitation chemistry, surface water chemistry and aquatic biota in acidified areas in Europe and North America from 1990 to 2008. NIVA-report SNO 6218/11. ICP Waters report 106/2011. Norwegian Institute for Water Research, Oslo. 126 pp.

Snucins, E., Gunn, J., Keller, B., Dixit, S., Hindar, A., Henriksen, A., 2001. Effects of regional reductions in sulphur deposition on the chemical and biological recovery of lakes within Killarney Park, Ontario, Canada. Environ. Monit. Assess. 67, 179-194.

Spiecker, H., Mielikäinen, K., Köhl, M., Skovsgaard, J., 1996. Growth Trends in Europe – Studies from 12 countries. Growth Trends in European Forests 5, 275-289.

Stoddard, J.L., Jeffries, D.S., Lükewille, A., Clair, T.A., Dillon, P.J., Driscoll, C.T., Forsius, M., Johannessen, M., Kahl, J.S., Kellogg, J.H., Kemp, A., Mannio, J., Monteith, D.T., Murdoch, P.S., Patrick, S., Rebsdorf, A., Skjelkvåle, B.L., Stainton, M.P., Traaen, T., Van Dam, H., Webster, K.E., Wieting, J., Wilander, A., 1999. Regional trends in aquatic recovery from acidification in North America and Europe 1980–95. Nature 401, 575–578.

Sverdrup, H., De Vries, W., 1994. Calculating critical loads of acidity with the simple mass-balance method. Water, Air, Soil Poll. 72, 143-162.

UBA, 2004. Manual on methodologies and criteria for modelling and mapping critical loads and levels and air pollution effects, risks and trends. Umweltbundesamt Texte 52/04, Berlin.

Wright, R.F., Alewell, C., Cullen, J.M., Evans, C.D., Marchetto, A., Moldan, F., Prechtel, A., Rogora, M., 2001. Trends in nitrogen deposition and leaching in acid-sensitive streams in Europe. Hydrol. Earth Syst. Sci. 5, 299-310.

Wright, R.F., Larssen, T., Camarero, L., Cosby, B.J., Ferrier, R.C., Helliwell, R., Forsius, M., Jenkins, A., Kopáček, J., Majer, V., Moldan, F., Posch, M., Rogora, M., Schöpp, W., 2005. Recovery of acidified European surface waters. Environ Sci. Technol. 39, 64A-72A.

Vuorenmaa, J., Holmberg, M., 2010. Relationships between critical load exceedances and empirical impact indicators. In: Kleemola, S. and Forsius, M. (Eds.) Convention on Long-range Transboundary Air Pollution International Cooperative Programme on Integrated Monitoring of Air Pollution Effects on Ecosystems. 19th Annual Report. Finnish Environment Institute. Helsinki, pp. 37-46.

Tables and Figures

Table 1. Exceedances of critical loads for acidification ($ExCL_A$) according to the historic scenario NAT2000 and mean annual concentrations and fluxes (2000-2002) of ANC, H^+, non-marine x(Ca+Mg) and xSO_4 in runoff water at 18 IM catchments. Negative exceedance values indicate that the critical loads are not exceeded. Runoff volume observations were not available at site AT01 (n.d.).

Site code	$ExCL_A$ (eq ha^{-1}yr^{-1})	ANC	H^+	x(Ca+Mg)	xSO_4	ANC	H^+	x(Ca+Mg)	xSO_4
		Concentration (µeq L^{-1})				Flux (eq ha^{-1} yr^{-1})			
AT01	-14160	3714	0.05	3871	64	n.d.	n.d.	n.d.	n.d.
CZ01	1500	443	0.10	1282	1162	311	0.07	810	723
CZ02	2097	-31	61	143	256	-198	411	783	1427
DE01	-241	126	0.84	198	63	1326	15	2423	849
EE02	-9204	2875	0.04	3055	311	2675	0.03	2930	333
FI01	-206	67	28	171	140	146	66	374	299
FI03	-676	124	0.50	96	25	387	1.9	300	81
GB01	40	56	0.43	43	27	274	4.6	225	149
LT01	-2074	2563	0.03	3829	1274	1507	0	2261	758
LT03	-1531	1015	0.09	1846	837	796	0.23	1985	1161
LV01	-5408	2388	0.05	2940	515	3431	0.12	4161	662
LV02	-7380	2258	0.06	2531	311	5019	0.13	5706	754
NO01	1001	-17	18	30	52	-346	304	286	666
NO02	-371	37	0.53	39	9.7	626	13	687	141
SE04	1187	-3.6	50	28	51	-29	299	206	371
SE14	583	82	31	136	126	213	112	477	513
SE15	497	-20	29	42	110	-150	188	223	650
SE16	-213	86	3.2	79	42	424	26	388	199

Table 2. Exceedances of critical loads of nutrient nitrogen ExCL$_{nut}$N and exceedances of empirical values of critical loads of nitrogen ExCL$_{emp}$N and mean annual (2000-2002) concentrations and fluxes of TIN (NO$_3$ + NH$_4$) in runoff water at IM catchments. Negative exceedance values indicate that the critical loads are not exceeded. Runoff observations were not available at all sites (n.d.).

Site code	ExCL$_{nut}$N (eq ha^{-1}yr^{-1})	ExCL$_{emp}$N (eq ha^{-1}yr^{-1})	TIN (µeq L^{-1})	TIN (eq ha^{-1}yr^{-1})
Number of sites	18	37	24	17
AT01	1117	710	101	n.d.
BY02	n.d.	42	85	n.d.
CZ01	1114	763	87	62
CZ02	1172	831	4.2	29
DE01	1140	902	103	1373
DE02	n.d.	736	12	n.d.
EE01	n.d.	804	45	n.d.
EE02	189	-144	71	71
FI01	56	42	5.7	13
FI03	-108	-101	1.6	5.7
FI04	n.d.	-191	0.9	n.d.
FI05	n.d.	-283	1.0	n.d.
GB01	-739	115	1.6	9.5
GB02	n.d.	3	22	n.d.
IS01	n.d.	-510	n.d.	n.d.
IT01	n.d.	556	n.d.	n.d.
IT02	n.d.	556	n.d.	n.d.
IT03	n.d.	1257	n.d.	n.d.
IT05	n.d.	551	n.d.	n.d.
IT06	n.d.	103	n.d.	n.d.
IT07	n.d.	1974	n.d.	n.d.
IT08	n.d.	1368	n.d.	n.d.
IT09	n.d.	391	n.d.	n.d.
IT10	n.d.	703	n.d.	n.d.
IT11	n.d.	657	n.d.	n.d.
IT12	n.d.	653	n.d.	n.d.
IT13	n.d.	806	n.d.	n.d.
LT01	465	383	11	7.4
LT03	699	653	17	27
LV01	680	523	30	54
LV02	275	222	13	32
NO01	442	498	9.2	116
NO02	-408	-108	2.2	36
SE04	660	329	3.7	27
SE14	534	53	5.5	19
SE15	210	157	2.0	11
SE16	-99	-166	1.6	5.7

Table 3. Average exceedances for sites not protected from acidification (AExCL) and eutrophication (AExCL$_{nut}$N, AExCL$_{emp}$N) and percentage of sites protected with different deposition scenarios.

	Total nr of sites	NAT2000	COB2020	Low*2020	MID2020	High*2020	MFR2020
AExCL$_A$ (eq ha^{-1}yr^{-1})	18	987	494	421	392	354	310
Acidification protection %	18	61 %	67 %	67 %	67 %	67 %	67 %
AExCL$_{nut}$N (eq ha^{-1}yr^{-1})	18	625	369	284	286	277	230
Eutrophication protection % mass balance critical load	18	22 %	28 %	28 %	33 %	39 %	39 %
AExCL$_{emp}$N (eq ha^{-1}yr^{-1})	37	578	349	238	221	177	154
Eutrophication protection % empirical critical load	37	19 %	35 %	38 %	41 %	41 %	54 %

Table 4. Correlations (Kendall Tau b correlation coefficients) of mean annual (2000-2002) concentrations and fluxes for ANC, xSO$_4$, H$^+$and TIN with exceedances of critical load for acidification (ExCL$_A$, NAT2000 scenario), exceedances of critical load of mass balance nutrient nitrogen (ExCL$_{nut}$N, NAT2000 scenario) and empirical critical load of nutrient nitrogen (ExCL$_{emp}$N, NAT2000 scenario). Statistically significant correlations (p < 0.05*, p < 0.01**, p < 0.001***) are highlighted in bold.

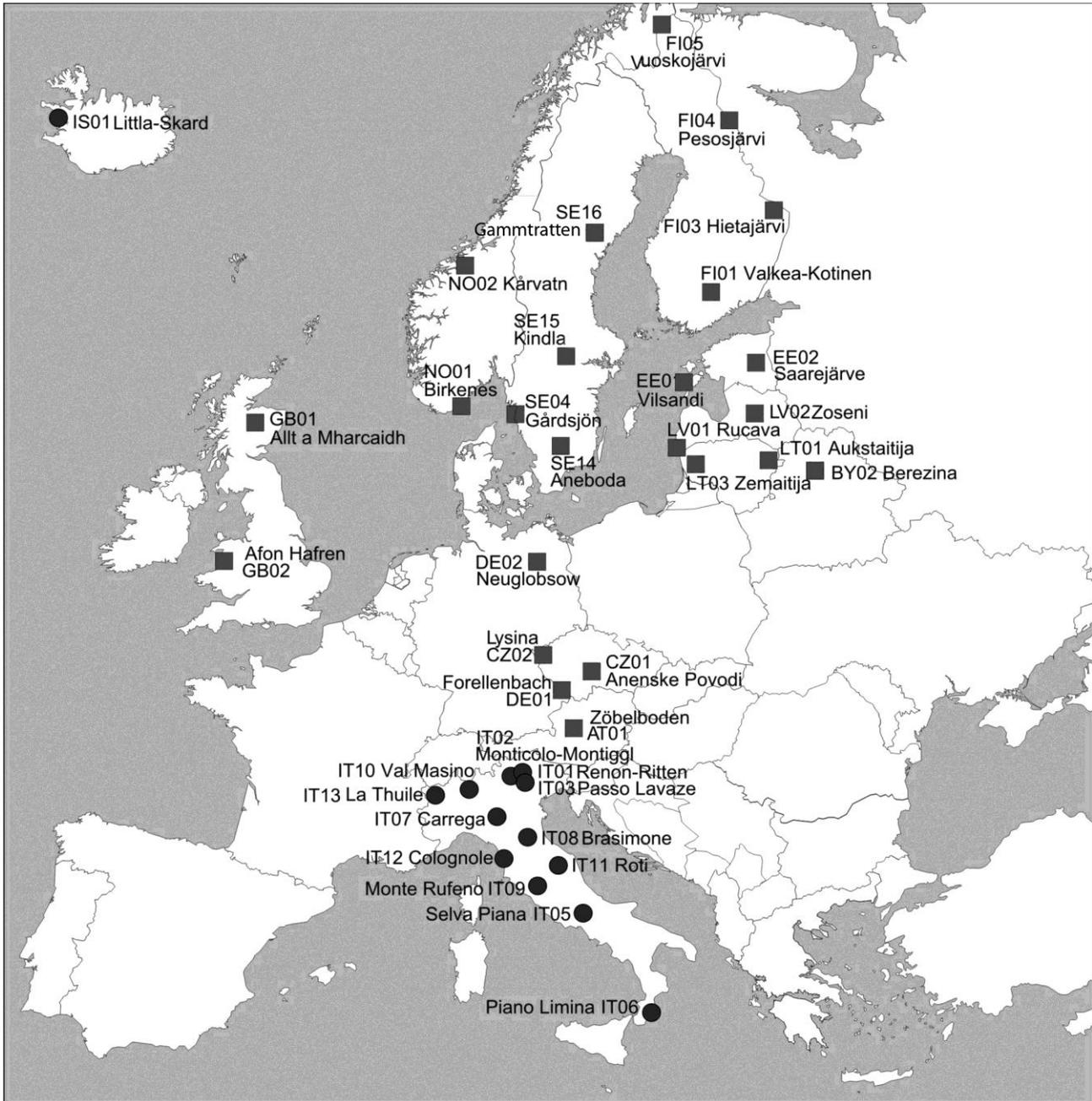|	ANC Mean Conc.	ANC Mean Flux	xSO$_4$ Mean Conc.	xSO$_4$ Mean Flux	H$^+$ Mean Conc.	H$^+$ Mean Flux	TIN Mean Conc.	TIN Mean Flux
ExCL$_A$	**-0.67*****	**-0.72*****	-0.06	0.13	**0.69*****	**0.66*****	-0.18	0.16
ExCL$_{nut}$N	0.11	-0.03	**0.39***	**0.71*****	0.08	0.09	**0.55****	**0.39***
ExCL$_{emp}$N	-0.04	-0.10	**0.32***	**0.66*****	0.13	0.07	**0.56*****	**0.43***

Figure 1. Location of the 37 ICP IM sites included in the critical load calculations. The catchments included in the comparison between exceedances of critical loads and runoff water concentrations and fluxes are indicated with a square (■).
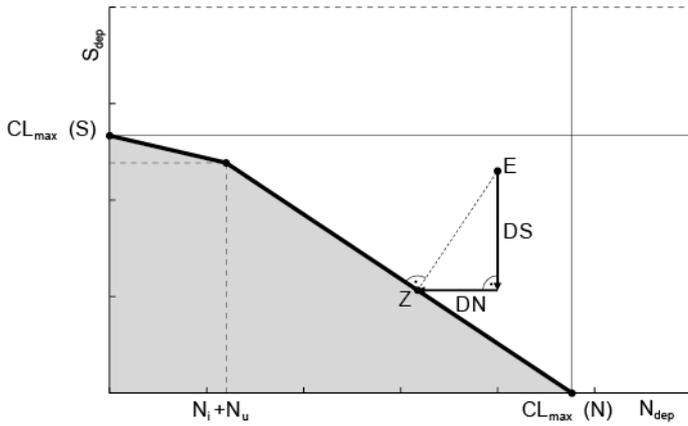
Figure 2. Piece-wise linear critical load function (CLF) of acidifying N and S for a lake or stream as defined by its catchment properties. For a given deposition pair (N_{dep},S_{dep}) the critical load exceedance is calculated by adding the N and S deposition reductions needed to reach the CLF via the shortest path (E→Z): Ex = ΔS+ΔN. The grey area below the CLF denotes deposition pairs for which the critical loads are not exceeded.

Figure 3. Acidification empirical impact indicators in relation to exceedance of critical loads. The x-axes show exceedance of critical load for acidification (ExCL$_A$, NAT2000 scenario) for aquatic ecosystems. The y-axes show annual mean concentrations (a, b) and fluxes (c, d) measured between 2000 and 2002 of ANC and H$^+$ in runoff for 18 ICP IM sites. Negative exceedance values indicate that the critical loads are not exceeded.
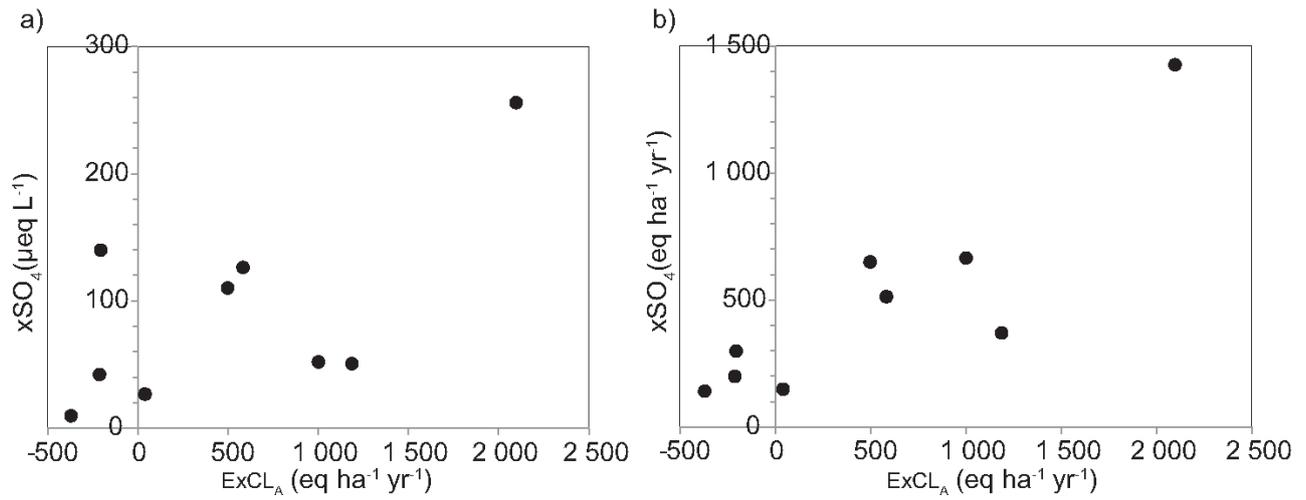
Figure 4. Acidification empirical impact indicators in relation to exceedance of critical loads at acid-sensitive catchments. The x-axes show exceedance of critical load for acidification (ExCL$_A$, NAT2000 scenario) for aquatic ecosystems at 9 acid-sensitive ICP IM catchments with ANC < 100 µeq L^{-1}. The y-axes show annual mean concentrations (a) and fluxes (b) of non-marine sulphate (xSO$_4$) measured between 2000 and 2002. Negative exceedance values indicate that the critical loads are not exceeded.
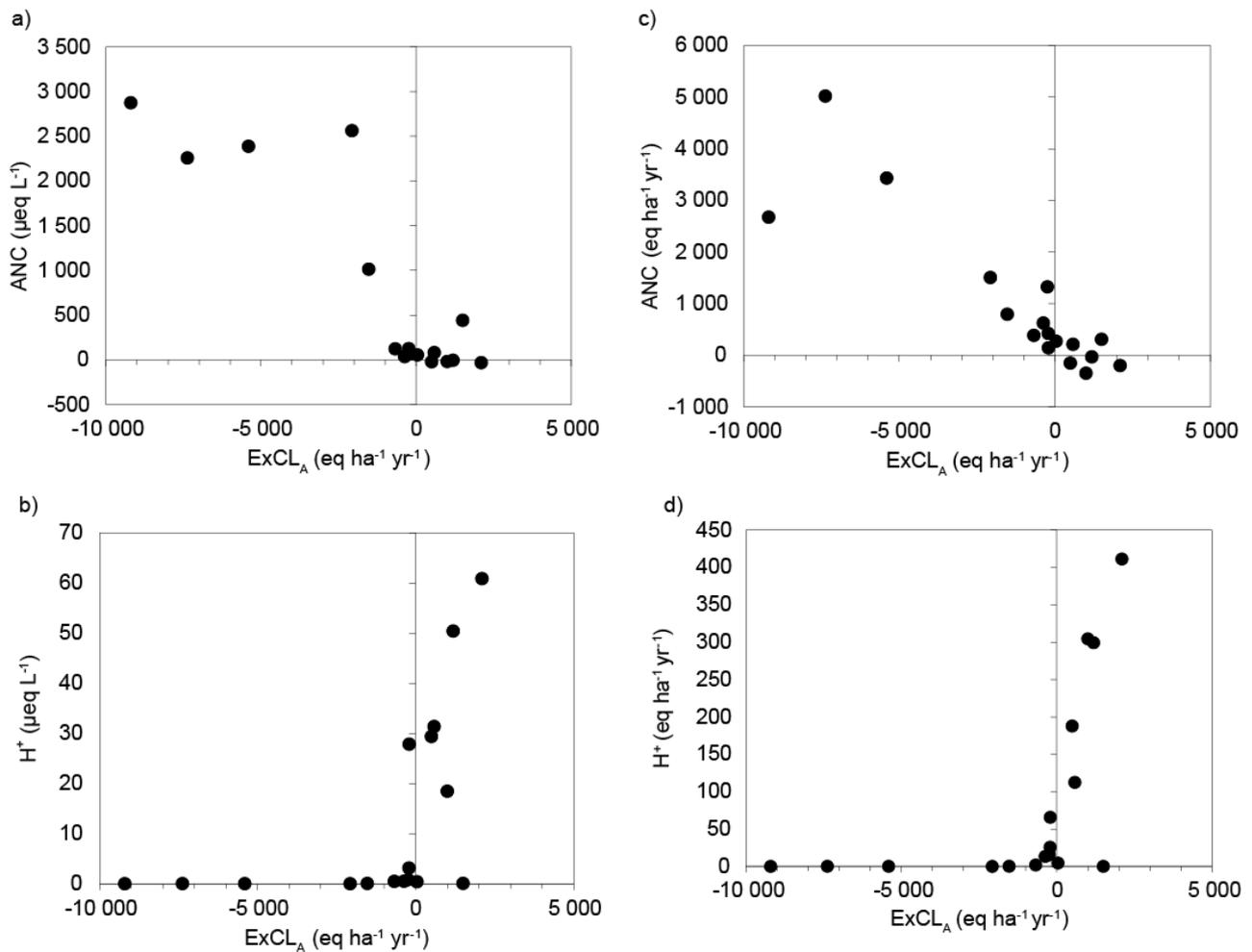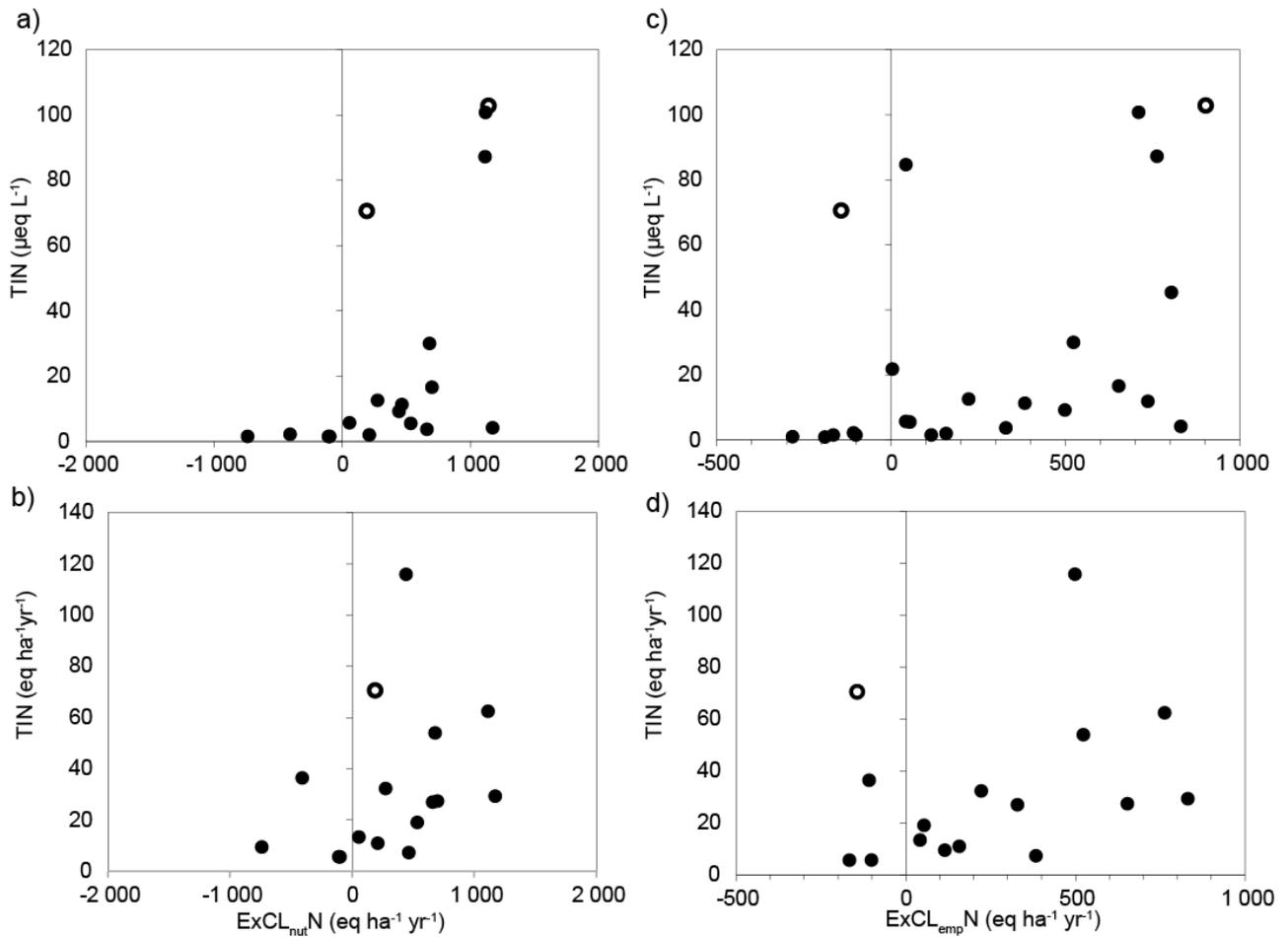
Figure 5. Eutrophication empirical impact indicators in relation to exceedance of critical loads of N. The x-axes show exceedances of mass balance critical loads of nutrient N (ExCL$_{nut}$N, NAT2000 deposition, a, b) and exceedances of empirical critical loads of nutrient N (ExCL$_{emp}$N, NAT2000 deposition, c, d). The y-axes show annual mean concentrations (a, c) and fluxes (b, d) measured (2000-2002 average) of TIN (=NO$_3$+NH$_4$) in runoff. Negative exceedance values indicate that the critical loads are not exceeded. Open circles indicate catchments with inputs of N from sources other than deposition. TIN flux for DE01 (1373 eq ha^{-1} yr^{-1}) is outside axis range and not shown in graphs.

Figure 6. TIN in relation to N deposition. The x-axes show N depositions (NAT2000 scenario) and the y-axes annual mean concentrations of TIN (=NO_3+NH_4) measured between 2000 and 2002 at 24 ICP IM sites (a) and annual mean fluxes of TIN measured between 2000 and 2002 at 16 ICP IM sites (b). Open circles indicate sites with inputs of N from sources other than deposition. The TIN flux for DE01 (1373 eq ha^{-1} yr^{-1}) is outside axis range and thus not shown.

Table A1. Properties of ICP IM catchments and vegetation plots as well as parameters used in the calculation of mass balance critical loads and empirical critical load values. Total catchment area (ha), area of lake (ha), fraction of peatland of terrestrial catchment area f_{peat}, acceptable concentration of N in soil solution $N_{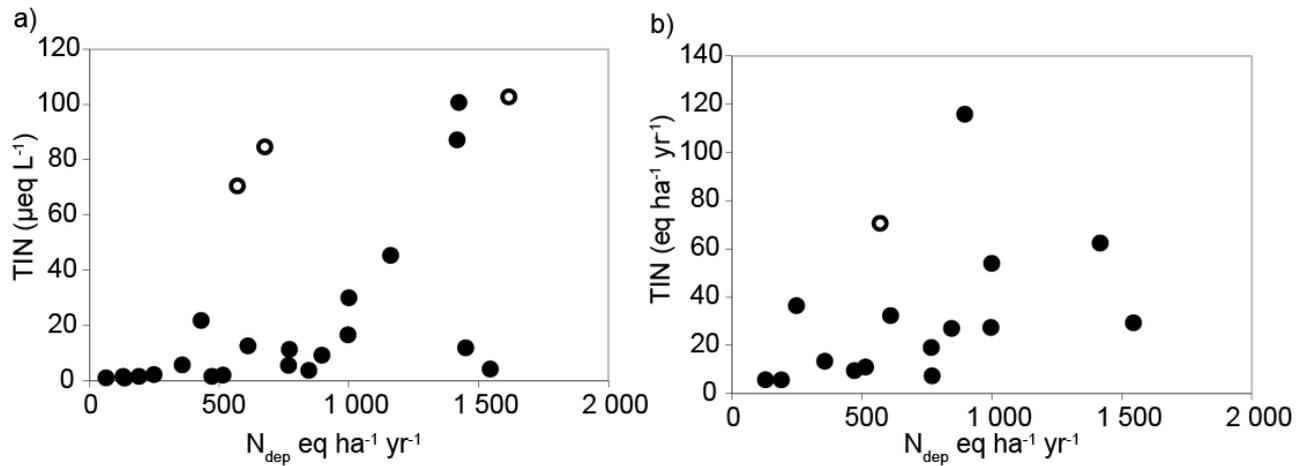acc}$ (mg L^{-1}), predominant vegetation per plot, area of vegetation plot (ha), EUNIS code, and empirical critical load of N $CL_{emp}N$ (kg ha^{-1} yr^{-1}).

Site		Total area (ha)	Lake area (ha)	f_{peat}	N_{acc} (mg L^{-1})	Predominant Vegetation per Plot	Plot Area (ha)	EUNIS code	$CL_{emp}N$ (kg ha^{-1} yr^{-1})
AT01	Zöbelboden	90	0	0	0.3	Spruce (*Picea abies*)	45	G3.1	10
						Beech (*Fagus sylvatica*)	45	G4	10
BY02	Berezina br.	72 600	-[a]	-[a]	-[a]	Boggy meadow	8 494	D1	5
						Coniferous forest	60 476	G4	10
CZ01	Anenske povodi	268	0	0	5.2	Alder (*Alnus*)	2.9	G1	10
						Ash (*Fraxinus excelsior*)	1.1	G1	10
						Beech (*Fagus sylvatica*)	5.4	G1	10
						Birch (*Betula*)	1.1	G1	10
						Larch (*Larix decidua*)	4	G1	10
						Lime (*Tilia*)	0.3	G1	10
						Maple (*Acer*)	0.3	G1	10
						Oak (*Quercus*)	0.3	G1	10
						Poplar (*Populus*)	0.5	G1	10
						Norway spruce (*Picea abies*)	205	G3.1	10
						Douglas fir (*Pseudotsuga menziezii*)	0.3	G3.1	10
						Fir (*Abies alba*)	1.9	G3.1	10
						Pine (*Pinus sylvestris*)	45	G3.4	5
CZ02	Lysina	27	0	0	0.8	Norway spruce (*Picea abies*)	19	G3.1	10
						Norway spruce (*Picea abies*)	8	G3.1	10
DE01	Forellenbach	69	1.4	0	0.5	Beech (*Fagus sylvatica*)	21	G1	10
						Spruce (*Picea abies*)	48	G3.1	10
DE02	Neuglobsow	2 140	-	-	-	Beech (*Fagus sylvatica*) and pine (*Pinus sylvestris*)	2 140	G4	10
EE01	Vilsandi	0.8	-	-	-	Scots pine (*Pinus sylvestris*)	0.8	G3.4	5
EE02	Saarejärve	332	27	0.1	2.0	Norway spruce (*Picea abies*) and Scots pine (*Pinus sylvestris*)	226	G3.1	10

FI01	Valkea-Kotinen	30	4	0.25	1.3	Norway spruce (*Picea abies*)	18	G3.A	5
						Scots Pine (*Pinus sylvestris*)	5	G3.A	5
						Norway spruce (*Picea abies*), Scots Pine (*Pinus sylvestris*), Birch (*Betula* spp.), Aspen (*Populus tremula*)	4	G4.2	5
FI03	Hietajärvi	464	106	0.35	1.0	Scots pine (*Pinus sylvestris*)	198	G3.A	5
						Birch (*Betula* spp.), Scots Pine (*Pinus sylvestris*)	15	G4.2	5
FI04	Pesosjärvi	636		-	-	Scots pine (*Pinus sylvestris*)	493	G3.A	5
						Norway spruce (*Picea abies*), Birch (*Betula* spp.)	31	G4.2	5
FI05	Vuoskojärvi	178	-	-	-	Mountain birch (*Betula pubescens* ssp *tortuosa*)	106	G1.9	5
						Scots pine (*Pinus sylvestris*), mountain birch (*Betula pubescens* ssp *tortuosa*)	24	G3.A	5
GB01	Allt'a Mharcaidh	998	0	0	1.5 [b]	Bog	200	D1	5 [c]
						Moss/lichen mountain summits	200	E4.2	5 [c]
						Sub-arctic heath/moor	499	F2	5 [c]
						Unmanaged conifers (pine)	100	G3.4	5 [c]
GB02	Afon Hafren	358	-	-	-	Acid grassland	107	E1.7	10 [c]
						Dwarf shrub heath	107	F4.11	10 [c]
ISO1	Litla-Skard	56	-	-	-	Level mire	3	D2	10
						Sloping mires	13	D4	15
						Grassland	4	E4	5
						Mossheath (*Racomitrium* spp.)	10	F2	5
						Birch (*Betula pubescens*)	15	G1	10
IT01	Renon-Ritten	0.3	-	-	-	Spruce (*Picea abies*)	0.2	G3.1	10
IT02	Monticolo-Montiggl	1.0	-	-	-	Oak (*Quercus*)	1	G1.8	10
IT03	Passo Lavaze	0.5	-	-	-	Spruce (*Picea abies*)	1	G3.1	10
IT05	Selva Piana	0.5	-	-	-	Beech (*Fagus sylvatica*)	1	G1.6	10
IT06	Piano Limina	0.5	-	-	-	Beech (*Fagus sylvatica*)	1	G1.6	10
IT07	Carrega	0.5	-	-	-	Oak (*Quercus petraea*)	1	G1.8	10
IT08	Brasimone	0.5	-	-	-	Beech (*Fagus sylvatica*)	1	G1.6	10
IT08	Monte Rufeno	0.5	-	-	-	Oak (*Quercus cerris*)	1	G1.8	10

IT10	Val Masino	0.5	-	-	-	Spruce (*Picea abies*)	1	G3.1	10
IT11	Roti	0.5	-	-	-	Oak (*Quercus cerris*)	1	G1.8	10
IT12	Colognole	0.5	-	-	-	Oak (*Quercus ilex*)	1	G2.1	10
IT13	La Thuile	0.5	-	-	-	Spruce (*Picea abies*)	1	G3.1	10
LT01	Aukstaitija	102	0	0	3.9	Birch (*Betula*)	1	G1	10
						Birch (*Betula*) and spruce (*Picea*)	8	G4	10
						Pine (*Pinus sylvestris*)	35	G3	5
						Spruce (*Picea*)	45	G3	5
						Spruce (*Picea*)-pine (*Pinus sylvestris*)	13	G3	5
LT03	Zemaitija	147	0	0	2.0	Birch (*Betula*)	4	G1	10
						Black alder (*Alnus glutinosa*)	0.3	G1	10
						Pine (*Pinus sylvestris*)	4	G3	5
						Spruce (*Picea*)	60	G3	5
						Spruce (*Picea*) and-pine (*Pinus sylvestris*)	75	G3	5
LV01	Rucava	665	7	0.2	1.7	Birch (*Betula pendula*)	239	G1	10
						Norway spruce (*Picea abies*)	93	G3	5
						Pine (*Pinus sylvestris*)	326	G3	5
LV02	Zoseni (Taurene)	27	1	0.3	1.5	Birch (*Betula*)	2	G1	10
						Norway spruce (*Picea abies*)	8	G3	5
						Pine (*Pinus sylvestris*)	16	G3	5
NO01	Birkenes	42	0	0	0.5	Aspen (*Populus tremula*)	2	G1	10
						Birch (*Betula*)	2	G1	10
						Norway spruce (*Picea abies*)	33	G3.A	5
						Pedunculate oak (*Quercus robur*)	1	G1	10
						Rowan (*Sorbus*)	0.2	G1	10
						Scots pine (*Pinus sylvestris*)	5	G3.B	5
NO02	Kårvatn	2 500	100	0	0.3	Scots pine (*Pinus sylvestris*) and alpine birch (*Betula nana*)	450	G4.2	5
SE04	Gårdsjön F1	4	0	0	0.8	Birch (*Betula*)	1	G1	10
						Norway spruce (*Picea abies*)	3	G3.1	10
						Pine (*Pinus sylvestris*)	1	G3.1	10
SE14	Aneboda	20	0	0.03	0.8	Mixed norway spruce (*Picea abies*) and -scots pine (*Pinus sylvestris*)	20	G3.1	10

| SE15 | Kindla | 19 | 0 | 0.03 | 0.8 | Norway spruce (*Picea abies*) | 19 | G3.A | 5 |
| SE16 | Gammtratten | 43 | 0 | 0.06 | 0.8 | Norway spruce (*Picea abies*) and pine (*Pinus sylvestris*) | 43 | G3.A | 5 |

[a] Area of lake, f_{peat} and N_{acc} given only for catchments used in mass balance critical loads analysis, for the other sites these variables are marked with '-' .

[b] This parameter is not used in the UK for mapping critical loads, as mass balance critical loads are calculated only for managed woodlands in the UK. For all other habitats, only empirical critical loads are used.

[c] The values used for mapping critical loads in the UK vary and are based on evidence of impacts (Hall et al. 2011).